

DETERMINATION OF SURGE TANK DIAPHRAGM HEAD LOSSES BY CFD SIMULATIONS

Détermination des Pertes de Charge d'un Diaphragme de Cheminée d'équilibre par Simulations Numériques

Sébastien ALLIGNE¹

Power Vision Engineering sàrl, Chemin des Champs-Courbes 1, CH1024 Ecublens, Switzerland
sebastien.alligne@powervision-eng.ch

Primoz RODIC

Hidroinstitut, Hajdrihova 28, SI-1115 Ljubljana, Slovenia, primoz.rodic@hidroinstitut.si

Jorge ARPE

AF-Consult Switzerland Ltd, Täfernstrasse 26, 5405 Baden-Dättwil, Switzerland, jorge.arpe@afconsult.com

Jurij MLACNIK

Hidroinstitut, Hajdrihova 28, SI-1115 Ljubljana, Slovenia, jurij.mlacnik@hidroinstitut.si

Christophe NICOLET

Power Vision Engineering sàrl, Chemin des Champs-Courbes 1, CH1024 Ecublens, Switzerland
christophe.nicolet@powervision-eng.ch

KEY WORDS

Surge Tank, Diaphragm, Head Losses, CFD, Transient Analysis.

ABSTRACT

At early stage of a hydroelectric project, 1D transient simulations are performed to determine the basic layout of power plant. In this phase, the design of surge tanks is decisive to achieve good dynamic performances of the power plant, with respect to water hammer and mass oscillations induced by the hydraulic machines for normal, exceptional and accidental operation. As the head losses between the gallery and the surge tank have strong influence on the transient behaviour of the hydraulic system they are usually optimized by means of 1D transient simulation to avoid low pressure in gallery or surge tank overflow. An asymmetric diaphragm is often placed at the surge tank inlet to achieve the optimum inlet and outlet head losses. Thus, the design of such diaphragm is a challenging task usually performed through an iterative process on reduced scale model. In this context, 3D CFD simulations can significantly improve the design process to select the appropriate geometry of the diaphragm. In this paper, head losses coefficients of a surge tank scale model are derived from CFD simulations performed with ANSYS CFX. Results are compared with measurements on reduced scale physical model and analytical approach. The good agreement of CFD computations with measurements demonstrates that a design optimization with 3D flow simulations can be performed preliminary to scale model tests in order to reduce the number of geometries to be tested to achieve the expected head losses.

¹ Corresponding author

1. INTRODUCTION

The design process of a hydroelectric powerplant layout includes 1D transient simulations aiming to avoid undesirable fluid transients during specific operational procedures. Many methods for controlling transients are available and the appropriate surge control devices are deduced from the transient simulations. For long pipeline systems, surge tanks are usually integrated in order to protect the headrace tunnel from water hammer induced by exceptional or accidental operations of the hydraulic machines. However, mass oscillations between surge tank and reservoir are experienced. Since the head losses between the headrace tunnel and the surge tank drives the transient behaviour of this mass oscillation [1], they are usually optimized by adding a singular loss through a diaphragm at the entrance of the surge tank.

The design of such diaphragm is a challenging task usually performed through an iterative process on reduced scale model. In this context, 3D CFD simulations can significantly improve the design process to select the appropriate geometry. Such numerical investigations have been performed previously by Huber [2] and Klasinc et al. [3] where they computed head losses coefficients of a diaphragm located in a T shape junction. Richter et al. [4] focused on the velocity field induced by the incoming jet into the surge tank and compared to PIV measurements. Regarding the optimization process of the diaphragm geometry, Gabl et al. [5] used CFD simulations and showed that theoretical approach gives different results. Similar investigations on geometries without diaphragm such as simple T-junction [6] or trifurcation [7], have been carried out to compute head losses coefficients.

This paper presents the design process of a surge tank diaphragm to be integrated into a pumped-storage power plant. First of all, the required head loss coefficients determined by 1D transient simulations for safety operating conditions are given. Then, physical model tests of the optimized geometry is presented with the head loss coefficients measurements. Finally, comparison with CFD simulations is performed in order to assess if 3D flow simulations can be used preliminary to scale model tests to reduce the number of geometries to be tested.

2. SURGE TANK DESIGN BY 1D TRANSIENT SIMULATIONS

The design of the surge tank of a pumped storage power plant is carried out by 1D transient simulations of the entire power plant as shown in Figure 1. This optimization procedure aims to find the surge tank geometry with the minimum volume and complying with the safety requirements of the waterways for normal, exceptional and accidental load cases. For this purpose, the optimisation of the head losses at the surge tank inflow and outflow could significantly contribute to minimize the size, and thus the cost of the surge tank, see [8]. Figure 2 shows simulation results of the transient behavior of the pumped storage power plant of Figure 1 obtained with the EPFL simulation software SIMSEN, see [9] for turbine and pump emergency shutdown which are usually one of the most critical cases to be considered in the design phase. It could be noticed that optimum head losses coefficients are achieved when maximum and minimum head, H , in the head race tunnel at the surge insertion, corresponds to the maximum and minimum water level, H_c , in the surge tank, see Stucky [1]. The final surge tank design should at least, ensure (i) to avoid emptying the surge tank and related risk of entrapped air in the waterways, (ii) prevent from water column separation in the gallery and top of the penstock, (iii) prevent from cavitation in the surge tank diaphragm if any, (iv) ensure sufficient mass oscillation damping, (v) comply with the turbine governor stability, see Thoma, [10], and (vi) prevent from overflow, if not permitted. Finally, the 1D transient simulation performed for the pumped storage of interest lead to an optimal inlet and outlet surge tank loss coefficient respectively equal to $K_{12}=5$ and $K_{21}=2.5$.

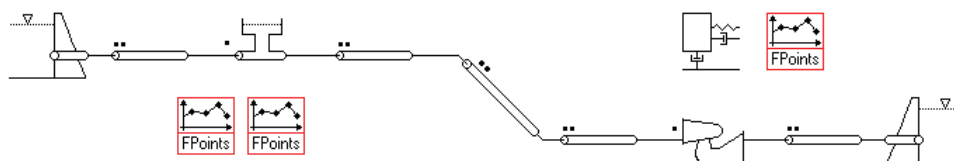


Figure 1: SIMSEN model of typical pumped storage power plant with upstream surge tank.

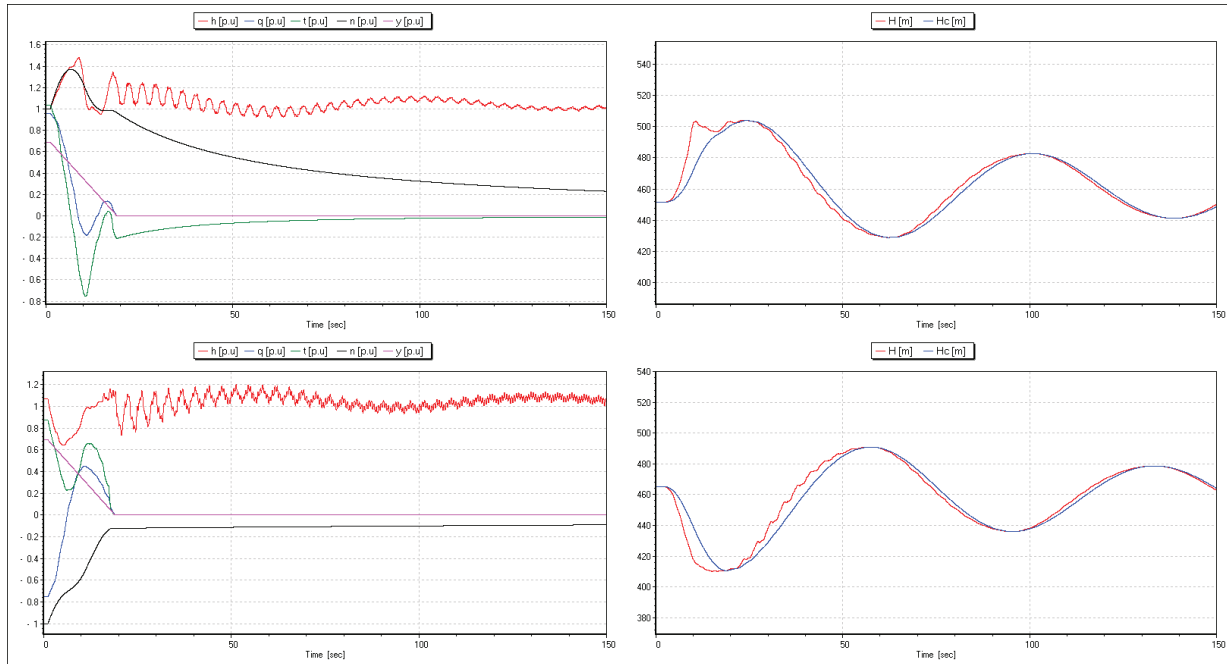


Figure 2: Simulation results of emergency shutdown of pumped storage in generating mode (top) and pumping mode (down) and transient behavior of the pump-turbine (left) and of the surge tank (right).

3. SURGE TANK DIAPHRAGM DESIGN BY PHYSICAL MODEL TESTS

3.1 Reduced Scale Model Geometry

After optimization of a pumped storage power plant surge tank by 1D transient analysis, experiments have been conducted at the Hydraulic Laboratory of Hidroinstitut, Ljubljana, to define the diaphragm geometry enabling to reach the specified surge tank head losses. Figure 3 shows the optimized geometry of the reduced scale model of the surge tank considering a length scale of $\lambda=1:13.2$.

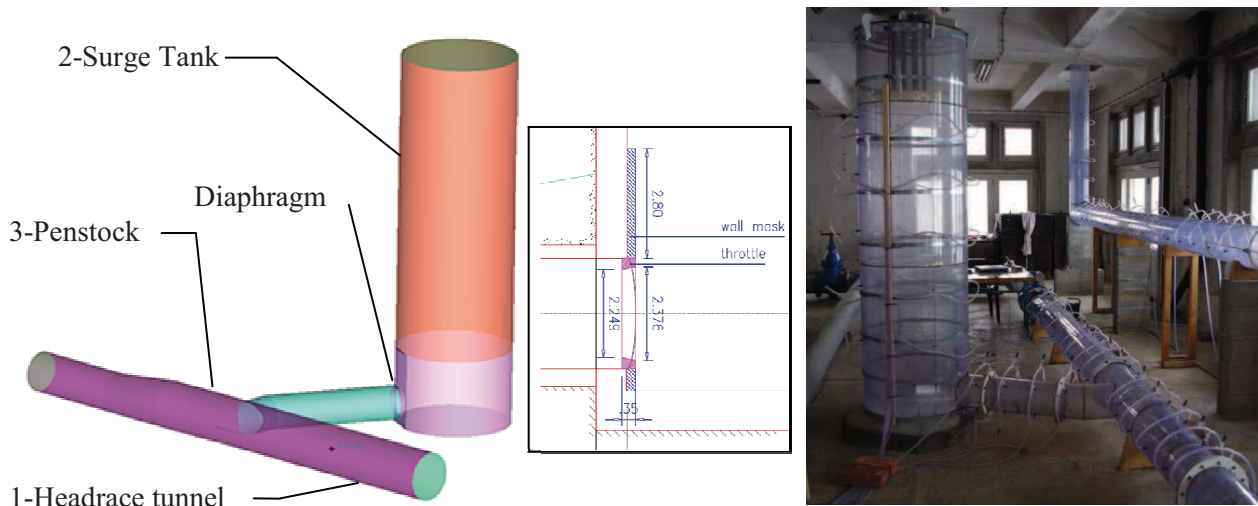


Figure 3: 3D reduced scale model geometry (left), drawing of the prototype diaphragm geometry (center) and experimental apparatus (right).

The pipe between the headrace tunnel and the surge tank features three singularities: a 90° T-junction, a change of direction and a diaphragm inducing sudden change of cross section. All these singularities contribute to the global head losses of the surge tank combined with the friction losses on the walls. For convenience, the headrace tunnel, the surge tank and the penstock are numbered respectively by 1, 2 and 3.

3.2 Investigated Operating Conditions

In this paper, four cases are investigated. These cases correspond to different operating conditions which differ according to the flow configurations in the system. Table 1 summarizes the investigated cases.

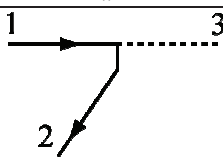
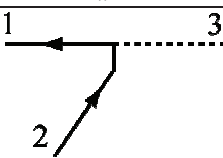
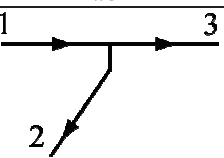
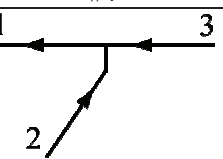
Case	#1	#2	#3	#4
Scheme				
Symbol	$1 > 2$	$2 > 1$	$1 > 2,3$	$2,3 > 1$
$\alpha_{q1} = Q_1/Q_{tot}$	1	1	1	1
$\alpha_{q2} = Q_2/Q_{tot}$	1	1	0.5	0.25
$\alpha_{q3} = Q_3/Q_{tot}$	0	0	0.5	0.75

Table 1: Investigated Operating Conditions.

Moreover, the distribution of the flow rates in each branch is mentioned by the flow rate ratio α_{qi} which is defined by the ratio between the flow rate in the considered branch i and the total flow rate. The flow configurations described in Table 1 correspond to the following cases:

- case #1: the flow is going from the headrace tunnel to the surge tank ($\alpha_{q1} = \alpha_{q2} = 1$) and the flow rate in the penstock is equal to zero ($\alpha_{q3} = 0$); this flow configuration is experienced during the mass oscillations between head race tunnel and surge tank consecutive to a turbine emergency shutdown;
- case #2: the flow is going from the surge tank to the headrace tunnel ($\alpha_{q2} = \alpha_{q1} = 1$) and the flow rate in the penstock is equal to zero ($\alpha_{q3} = 0$); this flow configuration is experienced during the mass oscillations between surge tank and head race tunnel consecutive to a pump emergency shutdown;
- case #3: the flow coming from the head race tunnel is equally divided into the penstock and into the surge tank ($\alpha_{q2} = \alpha_{q3} = 0.5$); this flow configuration is experienced in turbine mode just after an emergency shutdown;
- case #4: the flows coming from the surge tank and from the penstock are going to the headrace tunnel; for this case, most of the incoming flow comes from the penstock ($\alpha_{q2} = 0.25$, $\alpha_{q3} = 0.75$); this flow configuration is experienced in pump mode just after an emergency shutdown.

Respecting the Froude similitude with a length scale of the model λ , the scale factor for the Reynolds number transposition to prototype is equal to $\lambda^{3/2} = 48$. The involved Reynolds numbers are set in a range to ensure experimental head losses coefficients representative to the prototype conditions.

3.3 Experimental Setup

The reduced scale model of the surge tank is manufactured with clear PVC material. The headrace tunnel and the penstock in the vicinity of the T-junction are included in the reduced scale model geometry. The experimental setup is shown in Figure 4.

The model was equipped with electromagnetic flowmeters and measurements of piezometric heads were performed in 25 cross sections: 8 in the head race tunnel (Pz11-Pz18), 8 in the penstock (Pz31-Pz38) and 9 in the connecting pipe and the surge tank (Pz21-Pz29). To compute the head losses coefficients, reference cross sections, located far from flow disturbances, are selected: Pz15 in the headrace tunnel, Pz35 in the penstock, Pz28 in the surge tank for inflow conditions, Pz26 in the surge tank for outflow conditions.

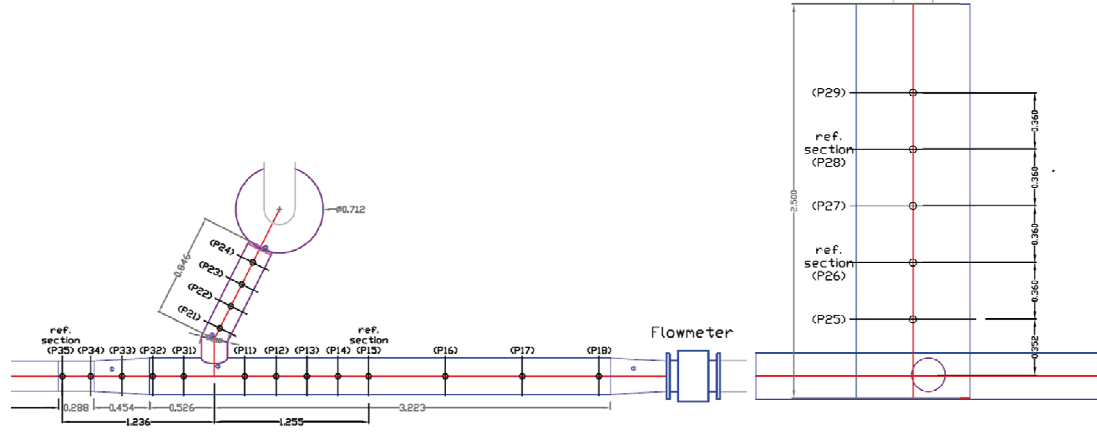


Figure 4: Experimental setup with top view (left) and side view (right) of the surge tank and related pressure taps.

3.4 Loss Coefficients

Head losses between sections i and j include both friction and singular losses. Hence, to derive the contribution of the singular part, the friction losses $\delta H_{ij_friction}$ must be subtracted to the total head difference $\Delta H_{ij} = H_i - H_j$, see Gardel [11]. The resulting singular head loss coefficient is defined by:

$$K_{ij} = (H_i - H_j - \delta H_{ij_friction}) / (Q_2^2 / 2gA_{ref}^2) \quad (1)$$

With Q_2 the reference flow rate and A_{ref} the reference cross section area corresponding to the connecting pipe between the surge tank and the headrace tunnel. The friction losses are estimated with the Darcy-Weisbach friction factor f as follows:

$$\delta H_{ij_friction} = f \frac{L}{D} \frac{Q^2}{2gA^2} \quad (2)$$

Preliminary measurements to derive the friction factor of the different pipe components are performed. The methodology consists in measuring the total head difference in a straight part of the considered pipe for several flow rates. Assuming a constant friction factor in the turbulent regime, a fitting function with the square of the flow rate is found to derive the coefficients. The friction factors f are given in Table 2.

Pipe	1-Headrace tunnel	2-Connecting pipe	3-Penstock
f	0.015	0.014	0.017

Table 2: Experimental Darcy-Weisbach friction factor f .

Finally, to derive the singular head losses coefficients, the same methodology as for the computation of the friction factors is used. Total head differences are measured for several flow rates and a fitting function is derived from raw data. The head losses coefficients are given in Table 3 for all the investigated cases.

Case	Symbol	K_{12}	K_{21}
#1	1>2	5.047	-
#3	1>2,3	5.274	-
#2	2>1	-	2.543
#4	2,3>1	-	1.370

Table 3: Experimental singular head losses coefficients K obtained by physical model tests.

4. CFD COMPUTATIONS OF DIAPHRAGM HEAD LOSSES COEFFICIENTS

4.1 Numerical Setup

For the present application, ANSYS-CFX 14.0 version is used for the flow computation in the surge tank reduced scale model. Steady Reynolds Averaged Navier-Stokes equations are solved and the set of

equations is closed with a eddy viscosity turbulence model: the Shear Stress Transport (SST) model which gives highly accurate predictions of the onset and the amount of flow separation. For this typical investigated geometry, flow separations are expected in the T-junction and at the outlet diaphragm. The computational domain is in adequacy with the reduced scale model and includes the reference cross sections used experimentally to compute the head losses. It is discretized with a structured mesh of 1.9 million nodes, generated with ANSYS ICEM 14.0. Influence of the mesh refinement was carried out in order to check the mesh independency on the head losses coefficients. Taking into account this spatial discretization, the "High resolution" advection scheme is used to solve the set of equations.

The inlet boundary condition is a prescribed velocity profile corresponding to a turbulent flow fully developed and obtained by a preliminary computation in a long straight pipe. Moreover, a non-slip wall condition is set up with a specified roughness. The roughness value is derived from the experimental Darcy-Weisbach factor f . Finally, for the outlet boundary condition, an opening condition is used. If the numerical model includes only one outlet, the "static pressure for entrainment" is set up. However, if the model features two outlets, for dividing flow conditions, one is setup as previously whereas for the other one, a specified velocity field is used to impose the flow rate.

4.2 Mesh Quality

Accuracy computation of head losses coefficients requires solving properly the boundary layer to predict wall friction and flow separations. Instead of using a very fine near wall grid and a low Reynolds model, the wall functions solution is used. The idea is to set the first computational node outside the viscous sublayer, and make suitable assumptions about the near-wall velocity profile. This meshing requirement is a decisive issue for the turbulence model performance. To set up the first computational node away from the wall, a non-dimensional wall distance from the wall y^+ is introduced. This distance should be between 20 and 200 to obtain a resolved boundary layer at least with 10 computational nodes. The y^+ area average is reported in Table 4 for the different simulated cases.

Case	Q_{tot}/Q_{ref}	\bar{y}^+
#1	1.53	84
#2	1.54	55
#3	1.56	63
#4	1.53	27

Table 4: Mesh quality analysis with y^+ values.

4.3 Loss Coefficients

Gravity being not applied in the numerical setup, total head in a given cross section is computed as:

$$H_i = \frac{1}{Q_i} \int_{S_i} \left(\frac{p}{\rho g} + \frac{\bar{C}^2}{2g} \right) \bar{C} \cdot \bar{n} \cdot dS \quad (3)$$

In the total head difference ΔH_{ij} derived from numerical simulations, part of the head losses are due to friction phenomena. Hence, to derive the singular head losses, the estimated experimental friction losses are subtracted. Indeed, the roughness value specified in the numerical set up has been calibrated with respect to experiments. For convenience, non-dimensional head losses Δh_{ij} are presented in the following charts:

$$\Delta h_{ij} = \frac{\Delta H_{ij} - \delta H_{ij_friction}}{\frac{Q_{2_ref}^2}{2gA_2^2}} \quad (4)$$

To define this non-dimensional value, the singular head losses are divided by a reference kinetic energy defined in the connecting pipe between the surge tank and the headrace tunnel with the nominal flow rate value of $Q_{2_ref} = 0.063 \text{ m}^3 \cdot \text{s}^{-1}$ which is relevant for our investigations. In Figure 5, head losses Δh_{ij} are plotted as function of the square of the non-dimensional flowrate of the connecting pipe $q_2 = Q_2/Q_{2_ref}$ for each investigated case.

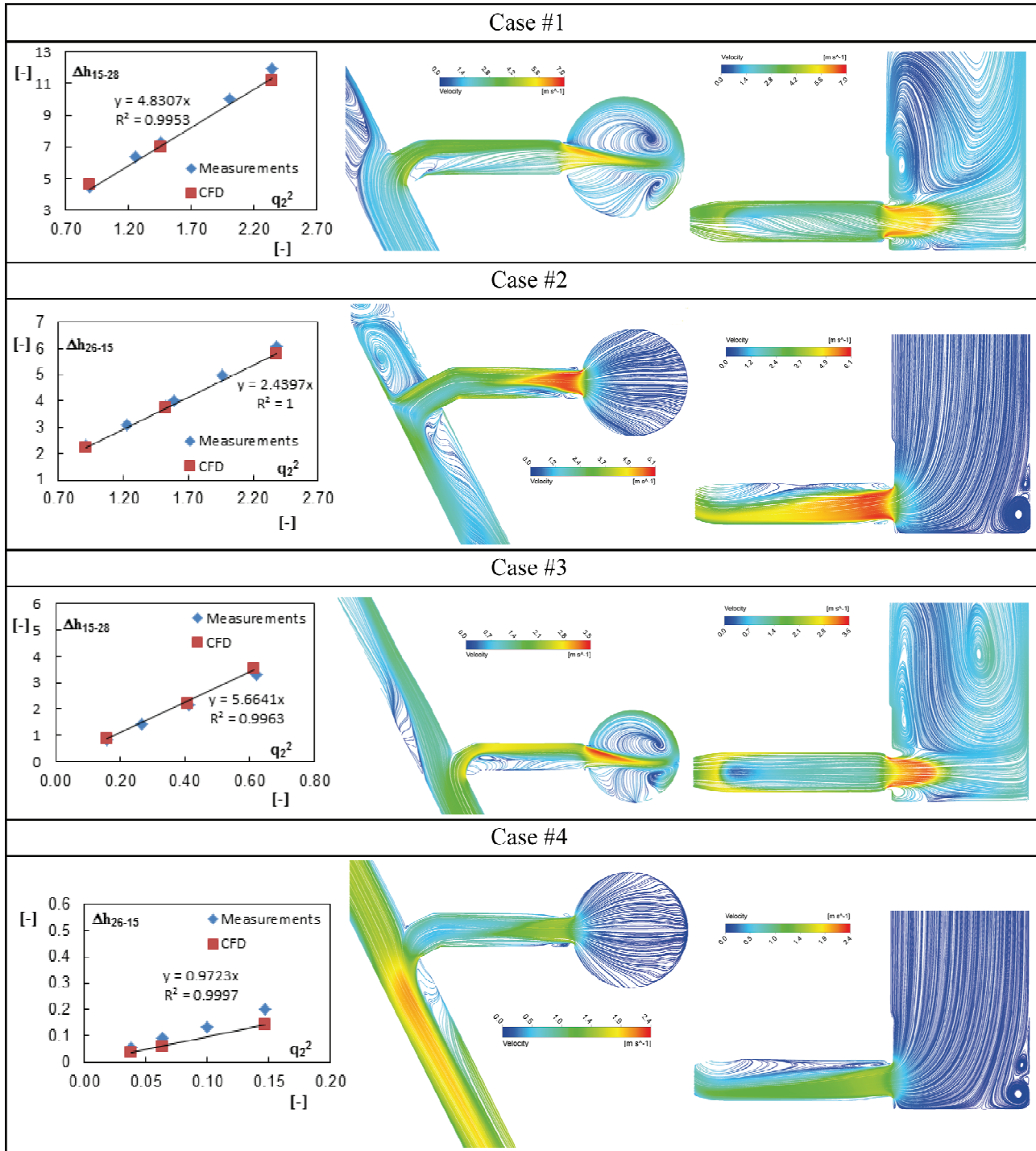


Figure 5: Head losses as function of the square flow rate (left), surface streamlines in the horizontal plane (center) and in the vertical plane (right).

The experimental methodology allowing to derive the singular head losses coefficients K_{ij} is used for the numerical approach. The head losses are computed for three flow rate values and are plotted as function of the square flow rate in order to fit numerical results with a linear function. The slope of this linear function gives the head loss coefficients K_{ij} . The comparison between experimental and numerical coefficients is given in Table 5,

Case	Symbol	Experimental		Numerical		Relative error
		K_{12}	K_{21}	K_{12}	K_{21}	
#1	1>2	5.047	-	4.830	-	-4.3 %
#3	1>2,3	5.274	-	5.664	-	+7.4 %
#2	2>1	-	2.543	-	2.440	-4.0 %
#4	2,3>1	-	1.370	-	0.972	-29 %

Table 5: Comparison between experimental and numerical head losses coefficients K .

For the three first cases good agreement is observed between experiments and flow simulations. However, a large relative error of 29% is observed for the case #4 where low Reynolds number in the connecting pipe is experienced with a value of $Re_2=1.10^5$. In that case the experienced head losses are very small. Indeed, regarding the absolute error for case #4, it corresponds to 0.9 cm of head losses whereas for case #1 the absolute error is 11.2 cm. In Figure 5, streamlines projected on the horizontal and the vertical planes are shown for each investigated case at the highest simulated flow rate. These visualizations allows to identify flow separations, swirling flow or large recirculations inducing the head losses in the system.

5. COMPARISON WITH THEORETICAL APPROACH

A comparison for cases #1 and #2 with theoretical approach can be performed with the Idel'cik handbook [12], taken as reference. For convenience, analytical formula are not written in this paper but the used diagrams are referenced. For case #1, the head loss coefficients for the T-junction and the diaphragm are derived respectively from the diagrams 7.21 and 4.11. Whereas for case #2, diagrams 4.12 and 7.16 are used. The obtained theoretical coefficients are given in Table 6 and compared to experimental and numerical results.

Case	Symbol	Experimental	Numerical	Theoretical
#1	1>2	5.047	4.830	5.16
#2	2>1	2.543	2.440	2.65

Table 6: Comparison between experimental, numerical and theoretical head losses coefficients K .

The theoretical approach gives as good results as numerical investigations contrary to Gabl et al. [5]. It can be concluded that the distance between the T-junction and the diaphragm, allows to compute separately the the head loss coefficients with analytical models. However, when the layout of the powerplant imposes a design far away from the analytical models such as diaphragm in T-junction [2] or sudden expansion downstream to a bend [5], the 3D flow simulations can be useful for preliminary design.

6. CONCLUSIONS

The present work shows the ability of steady RANS simulations to derive the head loss coefficients of a surge tank diaphragm under turbulent flow regimes. Hence, a design optimization with 3D flow simulations can be performed preliminary to scale model tests. Moreover, it is shown that theoretical approach gives as good results as numerical investigations when each component constituting the surge tank geometry can be considered separately. However, for complex geometries, the 3D flow simulations should be more accurate compared to the analytical models.

NOMENCLATURE

f	Darcy- Weisbach loss coefficient, [-]	H_i	Total head, [m]
g	Gravitational acceleration, [m.s ⁻²]	K_{ij}	Head loss coefficient, [-]
\vec{n}	Normal vector to surface, [-]	L	Length, [m]
p	Pressure, [Pa]	Pz_i	Piezometric head, [m]

q	Non-dimensional flow rate, [-]	Q	Flow rate, [m ³ .s ⁻¹]
y^+	Y plus, [-]	Re	Reynolds number, [-]
Δh_{ij}	Non-dimensional head losse from i to j , [-]	ΔH_{ij}	Total head loss from i to j , [m]
A	Cross section area, [m ²]	α_q	Relative flow rate, [-]
\vec{C}	Velocity vector [m.s ⁻¹]	λ	Length scale, [-]
D	Diameter, [m]	ρ	Density, [kg.m ⁻³]

ACKNOWLEDGEMENTS

Authors would like to thank particularly Mr. Roberto Rosseti from CADFEM company who placed test license of ANSYS products at our disposal to check feasibility of such study.

REFERENCES

- [1] Stucky, A. (1958). *Chambres d'équilibres*. EPFL, Cours d'aménagement des chutes d'eau, Sciences et Technique.
- [2] Huber, B. (2009). Physical Model Tests and CFD Simulation of an asymmetrical Throttle in a T-Shaped Junction of a High Head Power Plant. 33rd IAHR Congress: Water Engineering for a Sustainable Environment, pp. 5013-5021.
- [3] Klasinc, R., & Bilus, I. (2009). Experimental and Numerical Approach to Surge Tank Improvements. International Symposium on Water Management and Hydraulic Engineering.
- [4] Richter, W., Dobler, W., & Knoblauch, H. (2012). *Hydraulic and Numerical Modelling of an Asymmetric Orifice Within a Surge Tank*. 4th IAHR Intewrnational Symposium on Hydraulic Structures. Porto, Portugal.
- [5] Gabl, R., Achleitner, S., Neuner, J., Götsch, H., & Aufleger, M. (2011). *3D Numerical Optimisation of an Asymmetric Orifice in the Surge Tank of a High Head Power Plant*. 34th IAHR World Congress, Brisbane, Australia.
- [6] Huber, B. CFD Simulation of a T-junction.
- [7] Basara, B., Grogger, H. A., Klasinc, R., & Mayr, D. *Experimental and Numerical Study of the Flow Through a Trifurcation*.
- [8] Steyrer, P., (1999), Economic Surge Tank Design by Sophisticated Hydraulic Throttling, proceedings of the 28th IAHR congress, Graz, Austria.
- [9] Nicolet, C. (2007), Hydroacoustic Modelling and Numerical Simulation of Unsteady Operation of Hydroelectric Systems, PhD Thesis, EPFL n°3751, Lausanne, (<http://library.epfl.ch/theses/?nr=3751>).
- [10] Thoma, D., (1910), Zur Theorie des Wasserschlosses bei selbsttätig geregelten Turbinenanlagen, Munich (Oldenbourg).
- [11] Gadel, A., Rechsteiner, G. D., (1970). Les pertes de charge dans les branchements en Té des conduites de section circulaire. Bulletin technique de la Suisse Romande, N°25, pp. 363-391
- [12] Idel'cik, I.E. (1960). *Memento des pertes de charges*, Edition Eyrolles, Paris.